Lattice-Matched GaInAsSb/AlGaAsSb/GaSb Materials for Thermophotovoltaic Devices

C.A. Wang, C.J. Vineis*, H.K. Choi#, M.K. Connors, R.K. Huang

Lincoln Laboratory, Massachusetts Institute of Technology, Lexington, MA 02420-9108
**now at AmberWave Systems Corporation, Salem, NH 03079*
#now at Kopin Corporation, Taunton, MA 02780

L.R. Danielson, G. Nichols, G.W. Charache+

Lockheed Martin, Inc., Schenectady, NY 1230
+now at Princeton Lightwave, Cranberry, NJ 08512

D. Donetsky, S. Anikeev, G. Belenky

State University of New York, Stony Brook, NY 11794-2350

Abstract. High-performance GaInAsSb/AlGaAsSb/GaSb thermophotovoltaic (TPV) devices with quantum efficiency and fill factor near theoretical limits and open-circuit voltage within about 15% of the limit are reported. This paper discusses detailed studies of GaInAsSb epitaxial growth, the microstructure, and minority carrier lifetime that have led to these results. For further improvements in TPV cell performance, device structures with either a distributed Bragg reflector or a back-surface reflector are described.

INTRODUCTION

Recently, a thermodynamic analysis of thermophotovoltaic (TPV) system performance reported the importance of below-bandgap photon recuperation in determining tradeoffs between system efficiency and power density [1]. It was shown that the efficiency depends not only on the bandgap E_g of TPV cells but also on the reflectivity of the below-bandgap filter. The E_g where efficiency is a maximum decreases as filter reflectivity decreases. Thus, for TPV systems with radiator temperatures of approximately 1000 °C and a 95% reflective filter, a maximum efficiency was predicted for TPV devices with E_g of 0.5 eV [1].

GaInAsSb quaternary alloys have E_g that can be tailored from about 0.3 to 0.7 eV when lattice matched to GaSb substrates. Consequently, materials and device development for GaInAsSb TPV cells has been ongoing for several years [2-13], and devices have been demonstrated using structures prepared by all the major

CP653, *Thermophotovoltaic Generation of Electricity: 5th Conference*
edited by T. J. Coutts, G. Guazzoni, and J. Luther

epitaxial technologies, including liquid phase epitaxy [4-6], molecular beam epitaxy [7-8], and organometallic vapor phase epitaxy (OMVPE) [8-11]. This paper reports the current status of OMVPE-grown GaInAsSb TPV cells and the detailed studies that were performed to optimize GaInAsSb epitaxial layers for high-performance TPV cells. In addition, enhancements in performance by incorporating either a distributed Bragg reflector (DBR) [14] or back-surface reflector (BSR) [15] are discussed.

STATUS OF TPV CELL PERFORMANCE

A performance factor used for TPV device evaluation [1] is the diode efficiency η_{diode}, which is given by $\eta_{diode} = QE*F_0*(qV_{oc}/E_g)*FF$, where QE is the average internal quantum efficiency, F_0 is the usable fraction of thermal radiation with energy greater than the diode bandgap, qV_{oc}/E_g is the voltage factor based on electronic charge q, open-circuit voltage V_{oc}, and E_g of the diode material, and FF is the fill factor. Considering parameters that pertain specifically to diode performance, it was reported that theoretical limits for QE, qV_{oc}/E_g, and FF are 1, 0.7, and 0.7, respectively [2].

Figure 1 schematically shows a typical GaInAsSb/AlGaAsSb/GaSb TPV device structure that is being grown by OMVPE [8-11]. The GaInAsSb alloy composition corresponds to E_g of 0.52 to 0.55 eV. The structure consists of a thicker p-type emitter layer compared to the n-type base layer and an AlGaAsSb or GaSb window layer, and p-GaSb contact layer. This structure is used because shallow n-type contacts are difficult to prepare on GaSb-based materials and because of the larger minority carrier diffusion length in the p-type quaternary alloy compared to that in the n-type alloy. Surface recombination is detrimental to device performance [8], and both AlGaAsSb and GaSb window layers were shown to be effective in reducing interfacial recombination velocity [11].

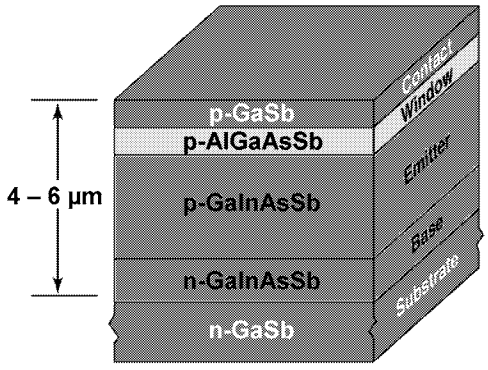

FIGURE 1. Schematic epitaxial GaInAsSb/AlGaAsSb/GaSb TPV device structure.

The spectral response for an uncoated TPV cell is shown in Figure 2. The data takes into account the measured surface reflectivity. Response is out to 2.5 μm, and QE is approaching the theoretical limit. Cell data of the peak value of EQE (uncorrected for surface reflection), V_{oc}, and FF for cells fabricated over several years are presented in Figures 3a, 3b, and 3c, respectively. The data are taken from uncoated cells in which the emitter layer thickness, emitter and base layer doping levels, window layers, and device fabrication techniques had been intentionally varied in an effort to study parameters influencing diode performance. The peak EQE and FF values currently approach theoretical limits, while the maximum voltage factor is 0.6.

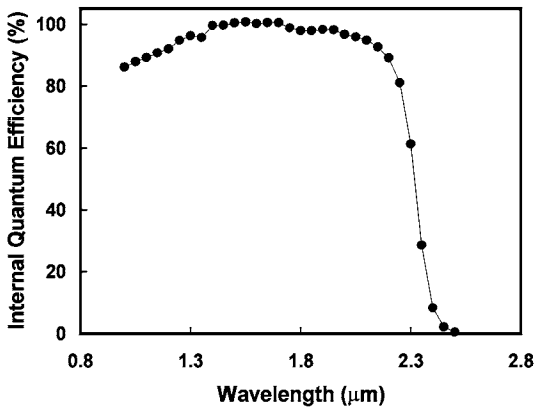

FIGURE 2. Spectral response of GaInAsSb/AlGaAsSb/GaSb TPV cell.

MATERIALS STUDIES

Factors that have a major impact on the quality of epitaxial GaInAsSb alloys, and thus TPV cell performance, include GaSb substrate quality, substrate preparation, and OMVPE growth parameters. Since the substrate is the template for epitaxial growth, its quality and preparation are extremely critical. GaSb substrates are less developed compared to the more conventional GaAs and InP III-V alloys, and the availability of high-quality GaSb substrates has been limited. GaSb is also a softer material, and thus, GaSb substrates are more susceptible to damage during substrate processing. Wafer bow is typically 10 μm and is considerably larger compared to only a few microns for GaAs. This bow can impact heat transfer during epitaxial growth and affect epilayer uniformity. In addition, a residue of SiO_2, which is used for substrate polishing, was sometimes observed on the GaSb surface by atomic force microscopy (AFM). This surface contamination will result in epitaxial defects. Thus, routine inspection of GaSb substrates quality is important.

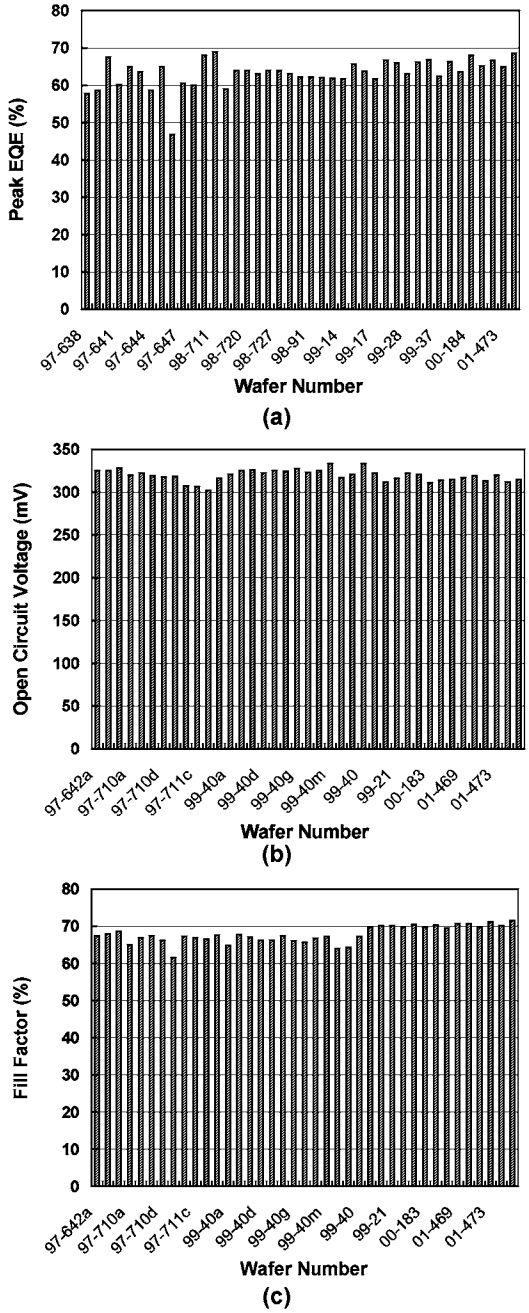

FIGURE 3. Device performance of uncoated GaInAsSb/(Al)Ga(As)Sb/GaSb TPV cells: (a) peak external quantum efficiency; (b) open-circuit voltage; (c) fill factor.

A critical step in substrate preparation is removal of gallium and antimony native oxides. Oxides can either be thermally evaporated in the growth reactor or chemically etched before introduction into the reactor. AFM images of GaSb grown either on an epi-ready substrate, where the oxide thermally evaporated, or on a chemically etched substrate are shown in Figures 4a and 4b, respectively. The morphology is rougher for the sample where the oxide was thermally evaporated. This is due to a thermally activated reaction between GaSb and antimony oxide, which consumes and thus roughens the surface [15]. When the oxide is chemically removed prior to loading into the reactor, there is negligible oxide and therefore, a smoother surface is achieved.

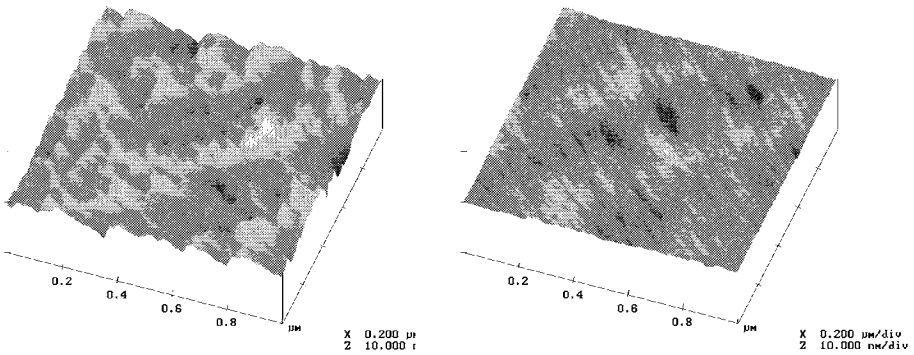

(a) (b)

FIGURE 4. Atomic force microscopy images of (a) GaSb grown on epi-ready GaSb substrate; (b) GaSb grown on chemically etched substrate.

OMVPE growth parameters were selected to minimize phase separation in GaInAsSb. Phase separation results in localized microscopic regions that are GaAs- and InSb-rich, and this inhomogeneity can degrade structural and electro-optical quality [11], and thus reduce minority-carrier recombination lifetime. Previously reported growth studies indicated that phase separation could be effectively limited by using low growth temperatures, high growth rates, and specific substrate orientations [11,17]. Such growth conditions reduce adatom surface diffusion during epitaxial growth.

Phase separation, however, cannot be completely eliminated because of thermodynamics, and an unusual manifestation of phase separation was observed. Figure 5a shows a cross-sectional transmission electron microscopy image of GaInAsSb with E_g of 0.5 eV. A natural superlattice (NSL) spontaneously formed at the onset of GaInAsSb growth. The observed contrast arises from a very small degree of strain associated with a modulation in composition in the vertical

direction. Figure 5b shows PL measurements at 4 and 300 K. Composition modulation is expected to increase the PL full width at half-maximum (FWHM) because of either layer thickness variations in the NSL or local variations in alloy composition. However, the PL data indicate FWHM of 9.5 meV, which is narrow for this alloy composition. The dependence of PL peak energy on temperature is similar to that observed for type-II band alignment [18]. Type-II alignment can enhance minority-carrier lifetime since electrons and holes are spatially separated [19]. However, if the alloy modulation results in material with E_g that is lower than the average alloy, the dark current would be higher.

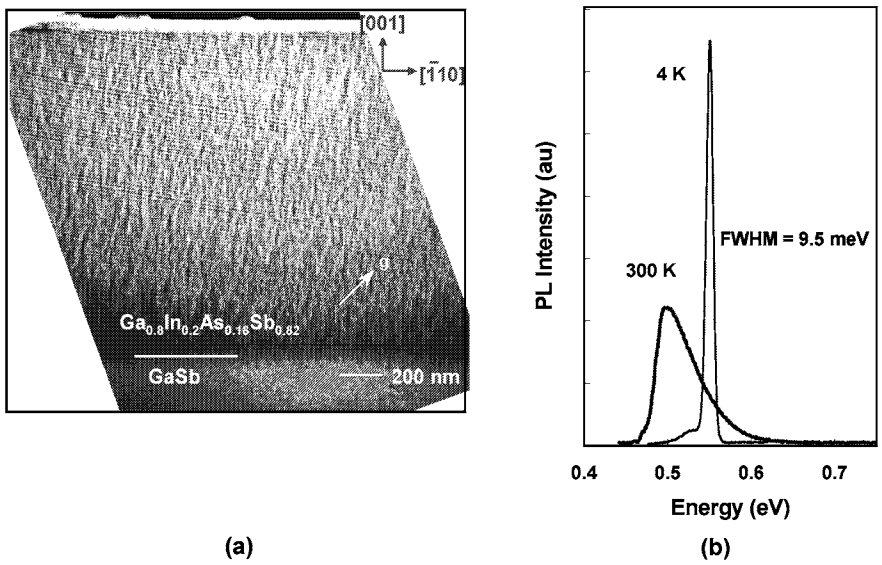

FIGURE 5. Natural superlattice in GaInAsSb: (a) cross-sectional transmission electron micrograph and (b) photoluminescence at 4 and 300 K.

Previously, it was suggested that the dominant bulk recombination mechanisms in GaInAsSb are radiative and Auger recombination and not Shockley-Read-Hall recombination [3,13]. The electron lifetime of p-GaInAsSb was measured by time-resolved PL [20]. Double-heterostructures with GaInAsSb doped at $2x10^{17}$ cm^{-3} were grown with different GaInAsSb thicknesses in order to separate the contributions of bulk and interfacial recombination processes according to the equation $1/\tau_{PL} = 1/\tau_{BLK} + 2S/W$, where τ_{PL} is the PL decay, τ_{BLK} is a bulk lifetime, S is the surface recombination velocity which is assumed to be equal at the front and back heterointerfaces, and W is the active layer thickness. In this approximation, S is assumed to be relatively small compared to the ratio of

minority carrier diffusion constant D to W (S<D/W), and photon recycling is negligible.

Three sets of samples were grown, each with different capping layers: nominally undoped p-GaSb ($1x10^{16}$ cm^{-3}), p-GaSb ($2x10^{18}$ cm^{-3}), and p-AlGaAsSb ($2x10^{17}$ cm^{-3}). The results are shown in Figure 6. All three plots demonstrate a linear dependence consistent with the equation. The structures with undoped p-GaSb cap layers resulted in the highest S of 3100 cm/s. In structures with p-GaSb cap layers doped to $2x10^{18}$ cm^{-3}, S was substantially smaller at 1140 cm/s. Thus, the use of a heavily doped cap layer makes it possible to suppress interfacial recombination. S was further reduced to 720 cm/s for structures with AlGaAsSb cap layers. Higher S values are due to accumulation of electrons at the GaInAsSb/GaSb type-II interface. Doping the cap layers reduces electron accumulation, while the AlGaAsSb cap layers results in no valence band offset [8]. Photon recycling can be significant and it can contribute to the slope and the offset. It was estimated that the contribution to S is about 200 cm/s for structures doped at $2x10^{17}$ cm^{-3}.

For nominally undoped p-GaInAsSb, photon recycling is negligible. The smallest S was 380 cm/s for undoped GaInAsSb (~$1x10^{16}$ cm^{-3}) with AlGaAsSb cap layers. In another set of samples, undoped GaInAsSb with undoped p-GaSb capping layers was also evaluated. Here a lower estimate of the bulk lifetime was determined to be 900 ns.

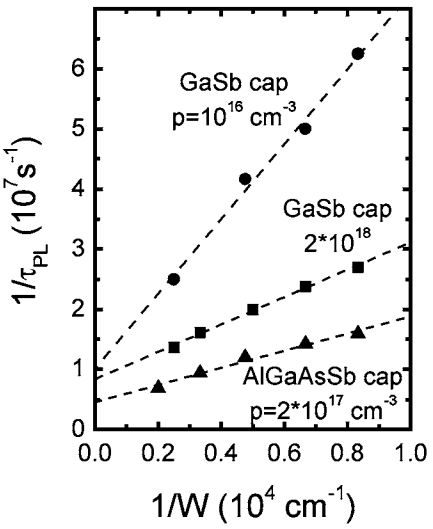

FIGURE 6. Inverse PL decay as a function of inverse thickness for three sets of GaInAsSb structures with different cap layers.

REFLECTORS FOR GaSb-BASED TPV DEVICES

Reflectors can enhance TPV performance by providing double-pass absorption for photons that are not absorbed in the first pass, especially near the band-edge. This allows for a thinner emitter layer and thus lower dark current. Furthermore, a reflector can enhance photon recycling and thus increase minority-carrier lifetime and V_{oc}. However, substrate absorption can reduce the effectiveness of a BSR [15], while increased series resistance can be problematic with DBR structures [21]. Preliminary results for both approaches are presented.

For either approach, low series resistance contacts and high shunt resistance R_{SH} are critical to device performance. Ohmic contacts to n- and p-GaSb were formed by depositing Au/Sn/Ti/Pt/Au and Ti/Pt/Ag/Pt/Au, respectively, and alloying the n-metal at 300 °C. The p-type contacts were not alloyed. The specific contact resistivity ρ_c was measured by the Cox-Strack method [22]. It was found that ρ_c for n- and p-contacts was 2.3×10^{-6} and 1.6×10^{-6} ohms-cm^2, respectively. It is slightly lower for the p-contacts than for the n-contacts because the Fermi level is pinned close to the valence band edge.

Large-area (0.5 cm^2) TPV cells were fabricated using a conventional photolithographic process. A single 0.15-mm-wide busbar connected to 10-μm-wide grid lines spaced 100 μm apart was used to make electrical contact to the front surface. TPV cells were defined by wafer sawing. The cutting introduces significant damage to the side walls and results in very low R_{SH} and degradation of FF. Saw-cut damage was removed with chemical etching, and it was found that the R_{SH} increased from a few ohms to hundreds of ohms, while the values for FF increased from below 60% to 70%.

GaInAsSb/GaSb TPV structures were grown with and without a five-period AlGaAsSb/GaSb DBR tuned to have reflectivity centered at 2.4 μm. The 300 K PL spectra for the TPV control structure without a DBR and the DBR/TPV structure are shown in Figure 7a. The PL intensity is enhanced by about 40%. The EQE of uncoated TPV and DBR/TPV devices is shown in Figure 7b. No enhancement in EQE near the band-edge was observed, which may be due to the narrow bandwidth (~400 nm) of the DBR centered at 2.4 μm. It is expected that increased EQE may be possible for TPV devices with a DBR centered at 2.2 μm. V_{oc} for the device with the DBR increased to 306 mV compared to 285 mV for the device without the DBR, or about 7%. Assuming a change only in recombination lifetime, a photon-recycling factor was estimated to be about 2.5. The series resistance for the cell with the DBR is slightly higher at 1.2×10^{-2} Ω, compared to 0.8×10^{-2} Ω without the DBR. Grading and doping the interfaces in the DBR structure should reduce the series resistance [21].

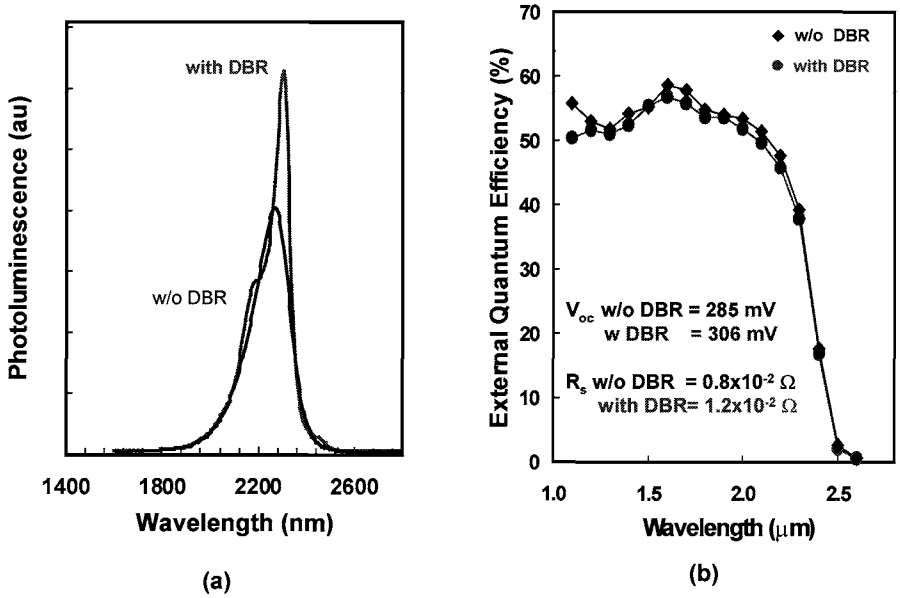

FIGURE 7. Comparison of GaInAsSb/GaSb TPV devices with and without distributed Bragg reflector: (a) 300 K PL spectra; (b) external quantum efficiency.

GaInAsSb/GaSb TPV devices were also fabricated with a BSR. Free-carrier absorption in the n-GaSb substrate can be reduced by thinning the substrate [15], and a reflectivity of nearly 90% through the GaSb substrate was measured for a substrate thinned to 100 μm thickness. A hybrid ohmic contact and BSR was constructed on the backside of a thinned and polished TPV cell. The EQE of an uncoated BSR-TPV device with substrate thickness of about 120 μm is shown in Figure 8. For comparison, the EQE of a conventionally processed TPV cell from the same wafer is also shown. The reflection limit of GaSb is also shown in the dotted-dashed line. In the wavelength regime from about 1.1 to 1.7 μm, the BSR-TPV cell and the reference cell have approximately the same EQE since the GaSb substrate is absorbing below 1.7 mm. From about 1.7 to 2.5-μm, the EQE of the BSR-TPV cell exceeds that of the reference cell, and indicates the enhancement due to the double-pass absorption. The peak difference in EQE is about 8% at a wavelength of 2.35 μm, which corresponds to a fractional increase in EQE of about 20% at this wavelength.

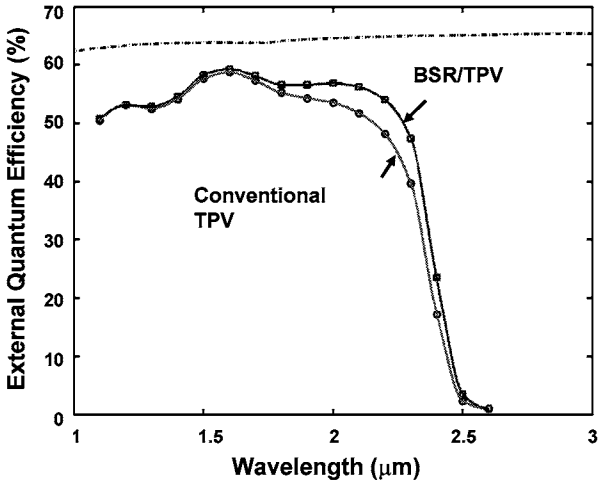

FIGURE 8. External quantum efficiency of GaInAsSb/GaSb TPV cells with and without back-surface reflector.

CONCLUSIONS

The optimization of GaInAsSb/(Al)Ga(As)Sb/GaSb TPV devices requires extensive effort in materials growth and characterization, device design, fabrication, and testing. High-performance TPV cells have been fabricated, indicating good control and reproducibility of both epitaxial growth and device processing. Values of EQE and FF are approaching theoretical limits, while the voltage factor is within 15% of the limit. Further improvements in the voltage factor should be forthcoming with increased understanding of recombination mechanisms in GaInAsSb. Preliminary device results on cells with a DBR structure indicate an increase in V_{oc}. Improvements in EQE was measured for TPV cells with a BSR.

ACKNOWLEDGMENTS

The authors gratefully acknowledge D.R. Calawa, J.W. Chludzinski, S. Hoyt, P.M. Nitishin, D.C. Oakley, and V.A. Todman for technical assistance. This work was sponsored by the Department of Energy under Air Force Contract No. F19628-00-C-0002. The opinions, interpretations, conclusions, and recommendations are those of the author and are not necessarily endorsed by the United States Government.

REFERENCES

1. P.F. Baldasaro, J.E. Raynolds, G.W. Charache, D.M. DePoy, C.T. Ballinger, T. Donovan, J.M. Borrego, J. Appl. Phys. **89**, 3319-3327 (2001).
2. G.W. Charache, J.L. Egley, D.M. DePoy, L.R. Danielson, M.J. Freeman, R.J. Dziendziel, J.F. Moynihan, P.F. Baldasaro, B.C. Campbell, C.A. Wang, H.K. Choi, G.W. Turner, S.J. Wojtczuk, P. Colter, P. Sharps, M. Timmons, R.E. Fahey, K. Zhang, J. Electron. Mater. **27**, 1038-1042 (1998).
3. G.W. Charache, P.F. Baldasaro, L.R. Danielson, D.M. DePoy, M.J. Freeman, C.A. Wang, H.K. Choi, D.Z. Garbuzov, R.U. Martinelli, V. Khalfin, S. Saroop, J.M. Borrego, R.J. Gutman, J. Appl. Phys. **85**, 2247-2252 (1999).
4. Z.A. Shellenbarger, M.G. Mauk, J.A. Cox, M.I. Gottfried, P.E. Sims, J.D. Lesko, J.B. McNeely, L.C. DiNetta, R.L. Mueller, 'Improvements in GaSb-Based Thermophotovoltaic Cells,' AIP Conf. Proc. 401, 117-128 (1997).
5. O.V. Sulima, R. Beckert, A.W. Bett, J.A. Cox, M.G. Mauk, IEE Proc.-Optoelectron. **147**, 199-204 (2000).
6. V.M. Andreev, V.P. Khvostikov, V.D. Rumyantsev, S.V. Sorokina, M.Z. Shvarts, 'Single-junction GaSb and tandem GaSb/InGaAsSb and AlGaAsSb/GaSb thermophotovoltaic cells,' Proc. 28th IEEE Photovoltaics Spec. Conf., 1265-1268 (2000).
7. V.B. Khalfin, D.Z. Garbuzov, H. Lee, G.C. Taylor, N. Morris, R.U. Martinelli, J.C. Connolly, 'Interfacial Recombination in In(Al)GaAsSb/GaSb Thermophotovoltaic Cells,' AIP Conf. Proc. 460, 247-255 (1999).
8. H.K. Choi, C.A. Wang, G.W. Turner, M.J. Manfra, D.L. Spears, G.W. Charache, L.R. Danielson, D.M. DePoy, Appl. Phys. Lett. **71**, 3758-3760 (1997).
9. C.A. Wang, H.K. Choi, D.C. Oakley, G.W. Charache, J. Cryst. Growth **195**, 346-355 (1998).
10. C.A. Wang, H.K. Choi, S.L. Ransom, G.W. Charache, L.R. Danielson, D.M. DePoy, Appl. Phys. Lett. **75**, 1305-1307 (1999).
11. C.A. Wang, H.K. Choi, G.W. Charache, IEE Proc.-Optoelectron. **147**, 193-198 (2000).
12. J.M. Borrego, S. Saroop, R.J. Gutman, G.W. Charache, T. Donovan, P.F. Baldasaro, C.A. Wang, J. Appl. Phys. **89**, 3753-3759 (2001).
13. S. Saroop, J.M. Borrego, R.J. Gutman, G.W. Charache, C.A. Wang, J. Appl. Phys. **86**, 1527-1534 (1999).
14. S.P. Tobin, S.M. Vernon, M.M. Sanfacon, A. Mastrovito, 'Enhanced Light Absorption in GaAs Solar Cells with Internal Bragg Reflectors,' Proc. 22nd IEEE Photovoltaics Spec. Conf., 147-152 (1991).
15. G.W. Charache, D.M. DePoy, P.F. Baldasaro, B.C. Campbell, 'Thermophotovoltaic Devices Utilizing a Back Surface Reflector for Spectral Control,' AIP Conf. Proc. 321, 339-350 (1996).
16. C.J. Vineis, C.A. Wang, K.F. Jensen, J. Cryst. Growth **225**, 420-425 (2001).
17. C.A. Wang, D.R. Calawa, C.J. Vineis, J. Cryst. Growth **225**, 377-383 (2001).
18. N.N. Ledentsov, J. Bohrer, M. Beer, F. Heinrichsdorff, M. Grundmann, D. Bimberg, S.V. Ivanov, B.Ya. Meltser, S.V. Shaposhnikov, I.N. Yassievich, N.N. Faleev, P.S. Kop'ev, Zh.I. Alferov, Phys. Rev. **B 52**, 14058-14066 (1995).
19. R.H. Ahrenkiel, S.P. Ahrenkiel, D.J. Arent, J.M. Olson, Appl. Phys. Lett. **70**, 756-758 (1997).
20. D. Donetsky, C.A. Wang, S. Anikeev, G. Belenky, S. Luryi, G. Nichols, 'Reduction of the Interfacial Recombination Rate in GaInAsSb/GaSb Heterostructures,' 44th Electron. Mater. Conf., 26-28 June 2002, Santa Barbara, CA.
21. K.Tai, L. Yan, Y.H. Wang, J.D. Wynn, A.Y. Cho, Appl. Phys. Lett. **56**, 2496-2498 (1990).
22. R.H. Cox, H.Strack, Solid-State Electron. **10**, 1213-1218 (1967).